

Kinetics of luminescence of isoelectronic rare-earth ions in III-V semiconductors

H. J. Lozykowski

*Department of Electrical and Computer Engineering, and Condensed Matter & Surface Sciences Program,
Ohio University, Athens, Ohio 45701*

(Received 30 November 1992; revised manuscript received 7 June 1993)

In this work we have developed a kinetics model of energy transfer from the host lattice to the localized core excited states of rare-earth isoelectronic structured traps (REI traps). The presence of low-lying empty core orbitals in rare-earth impurities introduces new excitation and recombination phenomena. To adequately describe the energy transfer to a REI trap, the buildup and decay kinetics of rare-earth luminescence, we consider six separate states of the REI impurity (unoccupied, electron occupied, electron occupied excited, exciton occupied, excited electron occupied, and excited exciton occupied). The energy-transfer processes occur through an Auger mechanism where the recombination energy of the bound electron with a free hole is transferred nonradiatively to the core states, or energy can be transferred from the bound exciton on a REI trap to the core states. If the initial and final states are not resonant (in both mechanisms), the energy mismatch must be accommodated by emission or absorption of phonons. Furthermore we discuss details of several quenching processes, which are incorporated into the kinetics equations. We derive two sets of differential equations for semi-insulating and *n*-type semiconductors governing the kinetics of rare-earth luminescence. Equations have been solved by a numerical method to derive the time dependence of the rise and decay kinetics as a function of excitation intensity. The numerically simulated luminescence rise and decay times show a good overall quantitative agreement with experimental data obtained for InP:Yb, over a wide range of generation rates.

I. INTRODUCTION

The investigation of the luminescence properties of rare-earth-doped III-V and II-VI semiconductors is of great interest both from the scientific and application points of view. The scientific interest is related to the uniqueness of optical and electrical properties of rare-earth impurities in semiconductor hosts. It is well known that rare-earth luminescence depends only slightly on the nature of the host and on the temperature. The $4f$ orbitals of rare-earth ions incorporated in semiconductors are so deeply buried within the electronic shell that the energy levels of the $4f^n$ configuration are only slightly perturbed compared to free ion energy levels. The electronic structure of the rare-earth luminescence centers and their electrical activities as well as their indirect photoluminescence and electroluminescence excitation mechanisms, are still not well understood. Among the rare-earth-doped III-V semiconductors, InP:Yb has been the most extensively studied.¹⁻⁹

Ytterbium in InP replaced indium on a substitutional site,^{10,11} and acts as an isoelectronic trap. It was originally proposed by Whitney *et al.*^{5(a)} and confirmed by others^{6,7,12(a)} that the Yb ion creates an electron trap at 30 meV below the bottom of the conduction band. Recently, admittance spectroscopy^{12(a)} was used to identify the electrical activity of Yb in *n*- and *p*-type InP. It was found that Yb in InP creates a hole trap at 50 meV above the valence band, and an electron trap at 29 meV below the conduction band. The 50-meV trap may be related to other impurities unintentionally incorporated into the crystal. This interesting result required confirmation using a sample grown by a more refined crystal growth

technique to ensure the high purity of the crystal. Recently it has been reported that Er in InP [Ref. 12(b)] and Yb in GaAs [Refs. 12(c) and 12(d)] introduced electron traps at 60 and 63 meV, respectively, below the conduction band. Colon *et al.*^{12(e)} investigated low-temperature photoluminescence, selectively excited luminescence, and deep-level transient spectroscopy on erbium-implanted GaAs. Conclusions of these measurements is that Er implantation introduces in GaAs two hole traps at 84 and 340 meV above the valence band. Several authors^{5(a),5(b),6,8,9,13(a),13(b)} have proposed a model that involves recombination of electron-hole pairs at the rare-earth (RE) traps to explain the excitation of RE core states.

In this paper we discuss only the structured isoelectronic traps in III-V semiconductors introduced by triply charged rare-earth ions replacing the element from column III (or another more complex RE isoelectronic traps). Furthermore, we develop the luminescence kinetic models that describe the energy-transfer and recombination processes. The presence of low-lying empty core orbitals in rare-earth impurities introduces new excitation and recombination phenomena, which will be discussed in detail. The RE luminescence rise time of the rare-earth-doped semiconductors, excited indirectly above the band gap, contain information about the energy-transfer processes from the host to the $4f^n$ electron system. It is shown that the study of the rise time at different temperatures, excitation intensities, and excitation pulse durations can provide important information about the energy-transfer, radiative, and nonradiative processes, respectively. The numerically simulated luminescence rise and decay profiles show a good quanti-

tative agreement with experiment over a wide range of generation rates. Finally, the possible quenching mechanisms and the temperature dependence of rare-earth luminescence are discussed.

II. THEORETICAL FORMULATION

It is well known that isoelectronic impurities in semiconductors produce bound states in the forbidden gap, binding an electron or a hole.^{14,15} An isoelectronic center can form bound states because of a short range central-cell potential. According to Thomas,¹⁵ the primary factors affecting the binding potential are the electronegativity and the size differences between the impurity and the host ion which it replaces. It is found experimentally that only very large atoms or very small atoms produce isoelectronic traps because they create large lattice distortion induced by the substitution. Thomas and co-workers^{16,15} have pointed out that to create a large binding potential, the substituted atom must generate a noticeable change in the local properties of the lattice. This is likely to produce an unfavorable free energy of the solution, and hence a rather low solubility can be observed. For instance, the maximum concentration seen for bismuth in GaP was less than 10^{18} cm^{-3} .¹⁷ Low solubility is also observed for rare earths in III-V semiconductors.¹⁸

Allen¹⁹ proposed different binding mechanisms for isoelectronic traps. According to Allen the isoelectronic impurity potential does not come from a pseudopotential difference of two isoelectronic atoms. Other possible sources are the spin-orbit coupling, and the strain field in the close vicinity of the impurity due to the size difference between the impurity and the host atom which it replaces. The main results of this theory are that the perturbing potential at an isoelectronic impurity may be attracted simultaneously to both the electron and the holes, so bound exciton states can occur without bound single-particle states. Baldereschi and Hopfield²⁰ have proposed a theory of isoelectronic traps assuming that the short-range potential arises from core differences, including spin-orbit interaction between the dopant atom and the host atom it replaces. The relaxation of the host crystal around the impurity as well as the screening model considered appear to be important for the binding energy. However, discrepancies between experimental binding energies and those calculated from the differences in the atomic pseudopotentials are observed. Excellent reviews of existing theories and experimental data of isoelectronic impurities were given by Baldereschi²¹ and Dean²² and Czaja.²³ In GaP two isoelectronic traps have been extensively investigated, namely a nitrogen electron trap, and a bismuth hole trap formed by substituting Bi and N for phosphorus.²² In the direct-band-gap III-V semiconductors, isoelectronic impurities have been investigated only in InP doped with bismuth.^{24,25} The neutral Bi, in a P site, creates a hole trap, and the isoelectronic complex (Bi,X)-(Bi,X) bound-excitonic molecules.²⁵ In II-VI semiconductors, ZnTe doped with oxygen-electron traps, and CdS doped with tellurium hole traps, were investigated in detail.²³

It is notable that all isoelectronic impurities discussed

above involve substitutions on the anion sites. The previous investigation²⁶ of cationic isoelectronic substituent (Mg, Ca, Sr, Ba) in ZnSe and ZnTe found no evidence of the presence of isoelectronic traps. A strong photoluminescence (PL) was reported recently from Mg-doped ZnSe [Refs. 27(a) and 27(b)] and ZnS (Ref. 28) which may arise from a new isoelectronic center generated by magnesium. We observed²⁷ sharp emission with a half-width of 16–60 meV (for $\text{Mg}_x\text{Zn}_{1-x}\text{Se}$, $x=0.04$), as required for exciton transitions at low temperatures. Furthermore the PL characteristics shift dramatically from deeper extrinsic emission in ZnSe to be dominated by narrow near-band-gap emission at all temperatures in the range 2–300 K in $\text{Mg}_{0.04}\text{Zn}_{0.96}\text{Se}$. The temperature dependence of the energy position of this peak follows the expected behavior for a free exciton transition in ZnSe. This peak remains strong in the PL spectrum all the way up to room temperature. This kind of behavior is not usually observed for bound exciton transitions related to neutral donor or acceptor centers. However, this behavior is typical for excitons bound to isoelectronic traps for which the dominant decay mode is radiative. The presence of the third electronic particle in the first two cases, but not in the third, was shown to introduce a dominant Auger decay mode for the bound exciton. In the Auger quenching, all the recombination energy is transferred to this third electronic particle that is expelled deep into the conduction (electron) or valence band (hole), respectively.

The striking feature of excitons bound to isoelectronic traps is a long luminescence decay time, ranging from a few hundred to a few thousand nanoseconds.^{25,29–33} The lifetimes of a neutral donor or acceptor bound excitons in direct-gap semiconductors are in the range of nanoseconds. For example the decay time of excitons bound to neutral donors or acceptors in InP are 0.5 and 1.5 ns, respectively.^{34(a)} The lifetime of an exciton bound to a neutral donor in GaAs is 1.07 ns.^{34(b)} In contrast the lifetime of an exciton bound to a Bi isoelectronic trap in InP is about 200 ns.²⁵

Table I shows that the outer electron configurations of RE^{3+} ions are the same ($5s^25p^6$). If the rare-earth ions replace the element from column III in III-V compounds that are isovalent concerning outer electrons of RE^{3+} ions (see Table I), they create isoelectronic traps in III-V semiconductors. This does not require association with other near distant charge compensating lattice defects or impurities, as is so common in II-VI semiconductors. The above conclusion is supported by the fact that the atomic covalent radii (ionic RE^{3+}) for all rare earths are bigger than atomic radii of Ga and In that they are replacing. Pauling's electronegativity of rare-earth elements is in the range of 1.1–1.25, and is smaller than Ga (1.81) and In (1.78) for which it substitutes. We know from different investigations that Yb substituted for In in InP behaves according to the above experimental rule and creates an isoelectronic trap. We have evidence that the other RE ions in III-V semiconductors can occupy different sites (not only substitutional). The rare-earth isoelectronic trap must not necessarily be the "pure" substitutional center, if the rare-earth ions are very active

TABLE I. Electron configuration of RE atoms, RE³⁺ ions (and some elements), ionic, covalent radii, and electronegativity.

Element	Electron configuration	Electron configuration RE ³⁺ & others	Ionic radius (Å)		Covalent radius (Å)	Electronegativity <i>a</i> : (Pauling's)
			2 ⁺	3 ⁺		
Cerium	4f ² 5s ² 5p ⁶ 6s ²	4f ¹ 5s ² 5p ⁶		1.02	1.65	1.12 ^a
Praseodymium	4f ³ 5s ² 5p ⁶ 6s ²	4f ² 5s ² 5p ⁶		1.00	1.65	1.13 ^a
Neodymium	4f ⁴ 5s ² 5p ⁶ 6s ²	4f ³ 5s ² 5p ⁶		0.99	1.64	1.14 ^a
Promethium	4f ⁵ 5s ² 5p ⁶ 6s ²	4f ⁴ 5s ² 5p ⁶		0.98	1.63	1.13 ^a
Samarium	4f ⁶ 5s ² 5p ⁶ 6s ²	4f ⁵ 5s ² 5p ⁶		0.97	1.62	1.17 ^a
Europium	4f ⁷ 5s ² 5p ⁶ 6s ²	4f ⁶ 5s ² 5p ⁶		0.97	1.85	1.20 ^a
Gadolinium	4f ⁷ 5s ² 5p ⁶ 5d ¹ 6s ²	4f ⁷ 5s ² 5p ⁶		0.97	1.61	1.20 ^a
Terbium	4f ⁹ 5s ² 5p ⁶ 6s ²	4f ⁸ 5s ² 5p ⁶		1.00	1.59	1.20 ^a
Dysprosium	4f ¹⁰ 5s ² 5p ⁶ 6s ²	4f ⁹ 5s ² 5p ⁶		0.99	1.59	1.22 ^a
Holmium	4f ¹¹ 5s ² 5p ⁶ 6s ²	4f ¹⁰ 5s ² 5p ⁶		0.97	1.58	1.23 ^a
Erbium	4f ¹² 5s ² 5p ⁶ 6s ²	4f ¹¹ 5s ² 5p ⁶		0.96	1.57	1.24 ^a
Thulium	4f ¹³ 5s ² 5p ⁶ 6s ²	4f ¹² 5s ² 5p ⁶		0.95	1.56	1.25 ^a
Ytterbium	4f ¹⁴ 5s ² 5p ⁶ 6s ²	4f ¹³ 5s ² 5p ⁶		0.94	1.74	1.10 ^a
Gallium	3d ¹⁰ 4s ² 4p			0.62	1.26	1.13 ^b
Indium	4d ¹⁰ 5s ² 5p			0.81	1.44	0.99 ^b
Zinc	3d ¹⁰ 4s ²		0.74		1.23	0.91 ^b
Cadmium	4d ¹⁰ 5s ²		0.97		1.48	0.83 ^b
Mercury	5d ¹⁰ 6s ²		1.10		1.49	0.79 ^b

^aElemental electronegativity in tetrahedrally coordinated environments (Ref. 35).

^bReference 36.

chemically, they can create a more complex center involving other impurity or native defects. The recent experimental data discussed in Sec. I shows that RE ions introduce electron or hole traps in III-V semiconductors, and we do not have evidence that RE ions act as donors or acceptors. The important roles of oxygen on RE luminescence have been discussed recently. Clearly we need more experimental and theoretical investigations devoted to rare-earth impurities to gain knowledge about the electrical activities of RE ions in semiconductors.

The rare-earth isovalent traps that we call isoelectronic "structured" impurities¹⁷ possess unfilled 4f^{*n*} core shells. The luminescence structure arises from intraconfigurational *f-f* transitions in the core of the isoelectronic "structured" impurities. The presence of low-lying empty core orbitals in rare-earth impurities introduces new excitation and recombination phenomena (which will be discussed in detail below). It distinguishes these impurities from the "simple" impurities (from the main group of elements of the Periodic Table). The "simple" impurity typically introduces only effective-mass-like states in the forbidden gap of the host crystals. According to Robbins and Dean,¹⁷ the formation of a bound state at the structured cationic isoelectronic impurities is fairly common, which is in contrast to the situation normally found for the anionic substituent in semiconductors discussed above.

The isoelectronic trap can be attractive either for electrons or for holes, and according to Allen's theory it can bind the exciton as a single entity. Since there is no charge involved, the isoelectronic center forms the bound states by a short-range central-cell potential. It is generally accepted that the formation of bound states is a specific property of the impurity and lattice combinations

discussed above. After an isoelectronic trap has captured an electron or a hole, the isoelectronic trap is negatively or positively charged, and by Coulomb interaction it will capture a carrier of the opposite charge, creating a bound exciton.

It has been well established that the "simple" isoelectronic traps can act as very efficient centers for radiative recombination in semiconductors. The structured isoelectronic cationic substitutional impurities (trivalent RE³⁺) in many phosphors lead to efficient characteristic luminescence.¹⁷ The trivalent rare-earth ions also create structured substitutional isoelectronic traps (REI trap) in some III-V semiconductors.

The "simple" isoelectronic center in III-V materials can exist in three possible states (to be identified later), instead of two as in the case of the Shockley-Read-Hall (SRH) recombination model.³² In the case of rare-earth isoelectronic traps the kinetics model is even more complicated because of energy-transfer processes between the localized state in the forbidden gap of the host, and the localized core states of structured isoelectronic impurities. There are three possible mechanisms of energy transfer. The first is the energy-transfer process from excitons bound to "structured" isoelectronic centers to the core electrons. It takes place as a result of the electrostatic perturbation between the core electrons of the "structured" impurity and the exciton effective-mass-like particle.¹⁷ This model is a modification of the Shaffer-Williams model of intrapair energy transfer to "structured" isoelectronic traps.³⁷ The second mechanism is transfer of energy to the core electrons involving the "structured" isoelectronic trap occupied by electron (hole) and free hole (electron) in the valence (conduction) band. The third mechanism is the transfer through an in-

elastic scattering process in which the energy of a free exciton near a "structured" trap is given to the localized core excited states.¹⁷ If the initial and final states are not resonant, the energy mismatch must be distributed in some way, e.g., by phonon emission or absorption.^{17,59(b)} According to Robbins and Dean,¹⁷ if the atomic core excitations are strongly coupled to the host phonons, the energy-transfer probability is likely to be higher. Strong phonon coupling may also be desirable in ensuring that relaxation down the ladder of core excited states occurs quickly, thus preventing back transfer. However, for efficient radiative recombination, the phonon coupling should not be strong, in order to prevent core deexcitation by nonradiative multiphonon emission. In this regard the rare-earth "structured" impurity seems to be ideal.

III. KINETIC MODELS

The SRH model that allows for only two possible states fails to give the correct general description of recombination kinetics of isoelectronic traps.³² The above discussion shows that isoelectronic impurities, both "simple" or "structured," can act as efficient centers for radiative recombination. The "simple" traps can exist in three possible states: (1) empty, (2) electron (hole) occupied, and (3) exciton occupied. In the case of RE^{3+} "structured" isoelectronic centers, the model is more complicated because the center can exist in six possible states. Furthermore the energy-transfer processes between the localized states in the forbidden gap and core states complicate the model. In our model, we assume that the isoelectronic trap is an electron trap such as Yb^{3+} in semi-insulating (SI) InP. When isoelectronic traps are present in n - or p -type materials the model will be different, especially at high temperature, and must be modified separately for n - and p -type material. The asymmetry between n - and p -type semiconductors results from the fact that the isoelectronic center binds only an electron (hole). Thus in an n -type material, a fraction of the isoelectronic traps will be occupied by electrons even before the sample is excited, while in p -type material all the isoelectronic electron centers will be empty.^{39,40} At low temperature (~ 4 K) there will be no difference between the n , p , or SI samples because the electrons or holes will be frozen. The donor and acceptor will act as "shunt" recombination centers. Figures 1–5 show the symbols' definitions, and physical models used in the kinetic analysis of the energy-transfer processes and recombination involving "structured" isoelectronic impurities. The proposed model accounts for energy transfer from the host to the core states through localized states in the forbidden gap, and for the dependence of the rise time on excitation intensities and temperature, including nonradiative recombination centers. In cases of n - or p -type semiconductors, we incorporate donor or acceptor centers to the model [see Figs. 1(d) and 1(e)].

By fitting the calculation to the experimental data, we can estimate important parameters related to energy transfer from the lattice to RE^{3+} centers, the Auger processes, temperature quenching mechanisms, and other

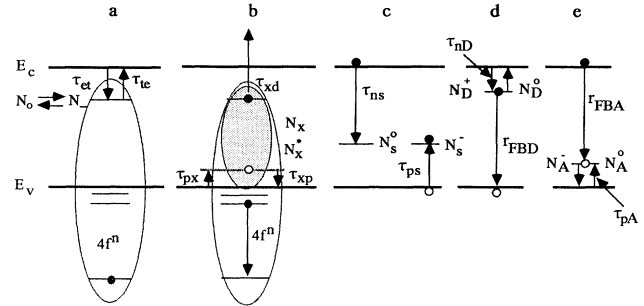


FIG. 1. Schematic diagram of recombination, trapping (thermalization), and exciton formation and dissociation processes involving structured rare-earth isoelectronic electron traps (represented by ellipse) with the atomlike $4f^n$ core states. (a) Trapping (liberation) τ_{et} (τ_{te}) of electron on REI traps. (b) Formation of exciton (shadow ellipse) by hole capture (τ_{px}); liberation of hole (τ_{xp}); dissociation of exciton (τ_{xd}) on the REI trap. (c) Shunt electron (hole) trapping time τ_{es} (τ_{ps}). (d) and (e) The trapping times for electron, τ_{nD} , and hole, τ_{pA} , by a donor (ionized), and an acceptor (neutral), respectively, and bound electron (hole) to free holes (electrons) recombination rates are $r_{FBD} = B_{FBD}(N_D^0)p$ [$r_{FBA} = B_{FBA}(N_A^0)n$].

important parameters that we discuss below. We take the depth of the Yb^{3+} REI trap (electron isoelectronic trap) from the experiment to be 30 meV below the conduction band, because we wish to apply results of the calculations to InP:Yb. This trap may exist in six distinct states: (1) the neutral unoccupied trap (concentration N_0), (2) the negatively charged (concentration N_-), (3) the exciton occupied (concentration N_X^0), (4) the neutral excited (concentration N_0^*), (5) the excited negatively charged (concentration N_-^*), and (6) the excited exciton occupied (concentration N_X^*). The total concentration of isoelectronic traps N is given by

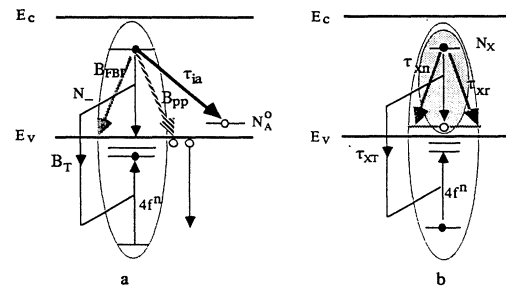


FIG. 2. A schematic representation of energy-transfer processes to core states of structured impurity and radiative and nonradiative transitions. (a) Auger energy-transfer process where the recombination energy of the bound electron with the free hole is transferred to the REI impurity core states (coefficient B_T). B_{pp} is the nonradiative Auger process coefficient involving bound electron and two free holes, B_{FBI} the coefficient of radiative recombination of bound electron to free hole, and τ_{ia} the recombination of bound electron with a hole on a distant acceptor. (b) The energy-transfer process from a bound exciton on a REI trap (shadow ellipse) to core states (B_{XT} transfer coefficient) and τ_{xr} and τ_{xn} are the bound exciton radiative and nonradiative recombination times, respectively ($1/\tau_2 = 1/\tau_{xr} + 1/\tau_{xn}$).

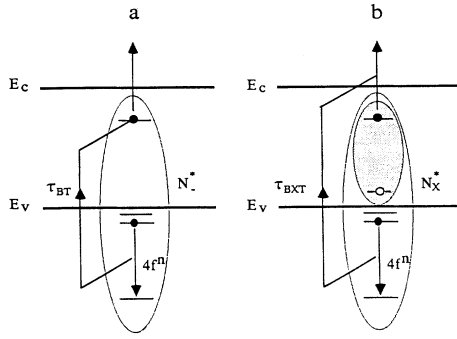


FIG. 3. Energy back transfer processes. (a) The auto deionization Auger quenching mechanism and its characteristic time τ_{BT} (Auger transfer rate $\tau_{BT} = B_{BT}N_-^*$). (b) The energy back transfer process from the excited REI trap to a bound exciton with characteristic time τ_{BXT} (Auger transfer rate $\tau_{BXT} = B_{BXT}N_X^*$).

$$N = N_0 + N_- + N_X + N_0^* + N_-^* + N_X^*.$$

Many of the symbols are the same as those defined in Refs. 31–33. Figure 1(a) shows how the neutral isoelectronic trap is transformed into an N_- state: an electron is captured within a time defined by $\tau_{et} = (v_{th}\sigma_{RE}N)^{-1}$, where v_{th} is the thermal velocity of the free electron, and σ_{RE} is the cross section for the capture of electrons by unoccupied traps. The capture rate of electrons by the isoelectronic trap is $(n/\tau_{et})(N_0/N)$, where n is the free electron density. The N_- center can be transformed to the neutral rare-earth core excited center N_0^* through an Auger process where the recombination energy of the bound electron with free hole is transferred nonradiatively to the core states with a rate

$$r_T = B_T N_- p,$$

where B_T is the energy-transfer coefficient, and p is the free hole density. If the initial and final states are not resonant, the energy mismatch must be distributed in some way such as phonon emission or absorption [Figs. 2(a) and 2(b)]. The N_- may also recombine radiatively or nonradiatively (via the Auger process) with a hole in the

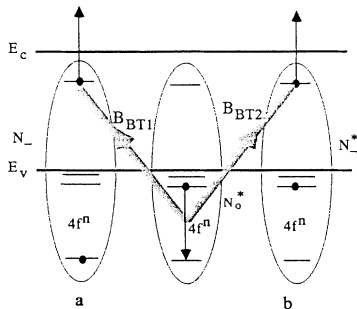


FIG. 4. Auger nonradiative recombination involving the interaction of the core excited REI trap (N_0^*) with an electron trapped on separate centers N_- (a) and N_-^* (b), where B_{BT1} and B_{BT2} are the Auger coefficients.

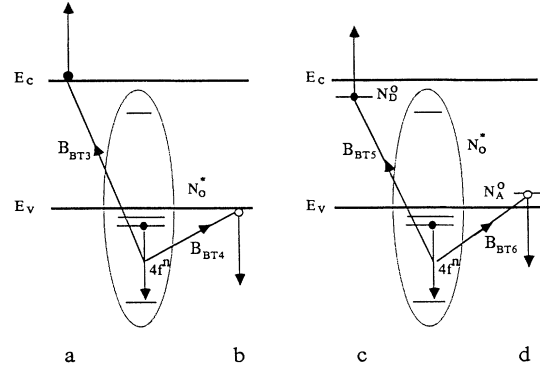


FIG. 5. Auger quenching processes involving interaction of the core excited REI trap with (a) and (b) free electrons or holes and their coefficients B_{BT3} and B_{BT4} . Interaction of the core excited REI trap with an electron (c) [hole (d)] on neutral donor (acceptor) and their coefficients B_{BT5} and B_{BT6} .

valence band with transition rate $r_{FBI} = B_{FBI}(N_-$ or $N_-^*)p$ and $r_{pp} = B_{pp}(N_-$ or $N_-^*)p^2$, respectively [Fig. 2(a)], or recombine radiatively with a hole trapped on a distant acceptor (in the case of p -type material). The last three processes transform the N_- center into the N_0 neutral trap. The N_0^* may capture an electron and be transformed into an N_-^* center. The N_-^* may lose the electron through processes described above, or by ion auto-deionization Auger process ($N_-^* \rightarrow N_0 + e$ -kinetic energy). This is the Auger nonradiative luminescence quenching mechanism of the excited rare-earth isoelectronic trap, with characteristic time τ_{BT} as shown in Fig. 3(a). The exciton bound to a REI trap with excited core states (N_X^*), can back transfer energy from core excitations to the exciton, and dissociate it with liberation of an electron or hole. Once formed, the N_- and N_-^* states can also be converted into N_0 and N_0^* states, respectively, by thermal ionization (time τ_{te}), or to N_X and N_X^* , respectively, by capturing a hole from the valence band with time defined by $\tau_{px} = (v_{th}\sigma_{Rx}N)^{-1}$ [see Fig. 1(b)].

The second important energy-transfer process from an exciton bound to a REI trap to core states is shown in Fig. 2(b). In this process energy is transferred from the bound exciton (on isoelectronic trap N_X) to the core states with the rate $r_{XT} = B_{XT}N_X$, where B_{XT} is the transfer coefficient, and τ_{XT} is the characteristic time. If the initial and final states are not resonant, the energy mismatch must be accommodated by emission or absorption of phonons. At sufficiently high temperatures, the electron from N_- and N_-^* may be thermally emitted to the conduction band at a rate $(n_t/\tau_{te})(N_-/N$ or $N_-^*/N)$, where $n_t = N_c\beta_t \exp[-E_{RET}/kT]$, $(1/\beta_t)$ is the degeneracy of the structured isoelectronic trap level at energy E_{RET} below the conduction band, and N_c is the conduction-band density of states.

The exciton bound to isoelectronic traps N_X and N_X^* can thermally dissociate by either of two processes: (1) it can dissociate into a free exciton (X) and neutral N_0 , or an neutral excited (N_0^*) REI trap, respectively; or (2) it can dissociate with the liberation of a hole, with the time

$1/\tau_{xp} = (1/\tau_{px})(p_h/N)$, where $p_h = N_v \beta_h^{-1} \exp[-E_h/kT]$, N_v is the effective density of state in the valence band, and β_h is the degeneracy of the hole component of the exciton having binding energy E_h .^{32,49}

The REI traps N_0^* , N_-^* , and N_X^* may also be deexcited to N_0 , N_- , and N_X , respectively, by desirable radiative transitions between the $4f^n$ core states, emitting photons with a decay time τ_3 .

The nonradiative decay channel of free carriers through an additional type of trap N_s , the "shunt path" with two states, is shown in Fig. 1(c). The concentrations of traps in these two states are denoted N_s^0 , the neutral unoccupied, and N_s^- , the negatively charged (bound electron), respectively ($N_s = N_s^0 + N_s^-$). The probability per unit time for an electron (hole) to be captured by an empty (electron occupied) shunt is $1/\tau_{ns}$ and $(1/\tau_{ps})$, respectively. For intrinsic excitation (band to band) the shunt paths deplete the excess electron-hole pairs. Under such excitation the shunt paths can be either partially or completely saturated, depending on the concentration, the time constants, and the generation rate of electron-hole pairs. Figures 1(d) and 1(e) show the characteristic parameters for donors and acceptors incorporated into the model, in cases of n - or p -type samples, respectively.

All the above discussed Auger processes [Figs. 4(a) and 4(b) and Figs. 5(a)–5(d)] are similar to the two center problems analyzed in some papers.^{32,50,41–43,51,45,46} Figure 4(a) shows an example of nonradiative recombination involving the interaction of a core excited isoelectronic trap (N_0^*) with an electron trapped on a separate center (N_-), or an electron trapped on a core excited REI trap (N_-^*). The recombination rates for these processes are proportional to N_0^* , and the concentrations of N_- or N_-^* traps such that

$$r_{BT1} = B_{BT1} N_0^* N_- , \quad r_{BT2} = B_{BT2} N_0^* N_-^* ,$$

where B_{BT1} , and B_{BT2} , are the Auger coefficients.

According to the theory developed by Langer,^{45,48} the two additional paths of energy transfer from the excited REI trap are the first to free electrons (holes) with Auger coefficients B_{BT3} (B_{BT4}), and second to electrons bound at the shallow donors (acceptors) [Figs. 5(a)–5(d)], and are also attributed to the luminescence quenching. The two processes shown in Figs. 5(c), and 5(d) involve interaction of a core-excited REI trap with an electron (hole) on a neutral donor (acceptor), and are characterized by Auger coefficients B_{BT5} and B_{BT6} , respectively. The first process is important during the exciting pulse, and the second processes are expected to be important at low temperatures where all electrons (holes) are frozen out onto neutral donors (acceptors).

We can now complete the formal description of the models by deriving the differential equations for the REI-trap energy-transfer processes and recombination kinetics. The differential equations govern the variations with the time of the concentrations of various components under band-to-band excitation. By consulting Figs. 1–5 (there are six possible states in REI traps, and two in shunt paths and generated free carriers), they may be readily written down:

$$\begin{aligned} \frac{dN_-}{dt} = & \frac{n}{\tau_{et}} \left[\frac{N_0}{N} \right] + \frac{N_-^*}{\tau_3} + \frac{1}{\tau_{xp}} \left[\frac{N_X}{N} \right] \frac{N_v}{\beta_h} \exp \left[-\frac{E_h}{kT} \right] \\ & - \frac{1}{\tau_{ie}} \left[\frac{N_-}{N} \right] \beta_i N_c \exp \left[-\frac{E_t}{kT} \right] \\ & - \frac{p}{\tau_{px}} \left[\frac{N_-}{N} \right] - B_{FBI}(N_-) p \\ & - B_T(N_-) p - B_{BT1}(N_0^*) N_- , \end{aligned} \quad (1)$$

$$\begin{aligned} \frac{dN_X}{dt} = & \frac{N_X^*}{\tau_3} + \frac{p}{\tau_{px}} \left[\frac{N_-}{N} \right] - N_X \left[\frac{1}{\tau_2} + \frac{1}{\tau_{XT}} + \frac{1}{\tau_{xd}} \right] \\ & - \frac{1}{\tau_{xp}} \left[\frac{N_X}{N} \right] \frac{N_v}{\beta_h} \exp \left[-\frac{E_h}{kT} \right] , \end{aligned} \quad (2)$$

$$\begin{aligned} \frac{dN_0^*}{dt} = & \frac{N_X}{\tau_{XT}} + B_T(N_-) p + \frac{1}{\tau_{ie}} \left[\frac{N_-^*}{N} \right] \beta_i N_c \exp \left[-\frac{E_t}{kT} \right] \\ & - \frac{n}{\tau_{et}} \left[\frac{N_0^*}{N} \right] - \frac{N_0^*}{\tau_3} - B_{BT1}(N_0^*) N_- \\ & - B_{BT3}(N_0^*) n - B_{BT4}(N_0^*) p , \end{aligned} \quad (3)$$

$$\begin{aligned} \frac{dN_-^*}{dt} = & \frac{n}{\tau_{et}} \left[\frac{N_0^*}{N} \right] + \frac{1}{\tau_{xp}} \left[\frac{N_X^*}{N} \right] \frac{N_v}{\beta_h} \exp \left[-\frac{E_h}{kT} \right] \\ & - \left[\frac{1}{\tau_3} + \frac{1}{\tau_{BT}} \right] N_-^* - \frac{p}{\tau_{px}} \left[\frac{N_-^*}{N} \right] \\ & - \frac{1}{\tau_{ie}} \left[\frac{N_-^*}{N} \right] \beta_i N_c \exp \left[-\frac{E_t}{kT} \right] \\ & - B_{BT2}(N_0^*) N_-^* - B_{FBI}(N_-^*) p , \end{aligned} \quad (4)$$

$$\begin{aligned} \frac{dN_X^*}{dt} = & \frac{p}{\tau_{px}} \left[\frac{N_-^*}{N} \right] - N_X^* \left[\frac{1}{\tau_2} + \frac{1}{\tau_3} + \frac{1}{\tau_{BXT}} + \frac{1}{\tau_{xd}} \right] \\ & - \frac{1}{\tau_{xp}} \left[\frac{N_X^*}{N} \right] \frac{N_v}{\beta_h} \exp \left[-\frac{E_h}{kT} \right] , \end{aligned} \quad (5)$$

$$\begin{aligned} \frac{dn}{dt} = & G + N_X^* \left[\frac{1}{\tau_{xd}} + \frac{1}{\tau_{BXT}} \right] \\ & + \left[\frac{N_- + N_-^*}{N} \right] \frac{1}{\tau_{ie}} \beta_i N_c \exp \left[-\frac{E_t}{kT} \right] \\ & + \frac{N_X}{\tau_{xd}} + \frac{N_-^*}{\tau_{BT}} - \frac{n}{\tau_{et}} \left[\frac{N_0 + N_0^*}{N} \right] - \frac{n}{\tau_{ns}} \left[\frac{N_s^0}{N_s} \right] \\ & + B_{BT2}(N_0^*) N_-^* + B_{BT1}(N_0^*) N_- , \end{aligned} \quad (6)$$

$$\begin{aligned} \frac{dp}{dt} = & G + \frac{1}{\tau_{xp}} \frac{N_v}{\beta_h} \exp \left[-\frac{E_h}{kT} \right] \left[\frac{N_X + N_X^*}{N} \right] \\ & - \frac{p}{\tau_{px}} \left[\frac{N_- + N_-^*}{N} \right] - \frac{p}{\tau_{ps}} \left[\frac{N_s - N_s^0}{N_s} \right] \\ & - B_T(N_-) p - B_{FB}(N_- + N_-^*) p , \end{aligned} \quad (7)$$

$$\frac{dN_s^0}{dt} = \frac{p}{\tau_{ps}} \left[1 - \frac{N_s^0}{N_s} \right] - \frac{n}{\tau_{ns}} \left[\frac{N_s^0}{n_s} \right], \quad (8)$$

$$N_0 = N - N_- - N_X - N_0^* - N_-^* - N_X^*, \quad (9a)$$

$$N_s = N_s^0 + N_s^-, \quad (9b)$$

$$p = n + N_- + N_-^* + \left[1 - \frac{N_s^0}{N_s} \right] N_s. \quad (10)$$

Equations (1)–(5) govern the negatively charged-rare earth isoelectronic trap populations (1), the neutral exciton occupied rare-earth isoelectronic trap populations (2), the neutral core excited rare-earth isoelectronic trap populations (3), the negatively charged core excited rare-earth isoelectronic trap populations (4), and the exciton occupied core excited rare-earth isoelectronic trap populations (5), respectively. Equations (6) and (7) represent the changes in the total free electron (n) and hole (p) populations, respectively. Equation (8) governs the density of shunt path traps. Equations (9a) and (9b) state the constancy of the total concentrations of REI traps and shunt paths, respectively, and Eq. (10) is the neutrality condition equation. $G = gf(t - T)$ is the generation rate of free electrons and holes by above band-gap laser excitation. The electron-hole pair generation rate is controlled by a unit step function $f(t - T)$, (T is the pulsewidth) which takes on the value of zero or unity according to whether its argument is less than or equal to zero or greater than zero. The volume generation rate is approximated by $g(z) \cong \alpha I \exp[-\alpha z]$, where α is the absorption coefficient, and I is photon flux in # photons/(cm²/sec).

For n -type material the equations are even more complicated (see the Appendix); similar equations hold for p -type material. Such systems of coupled, first-order stiff nonlinear differential equations require specialized numerical integration routines designed specifically for stiff systems. The kinetic equations were solved numerically as a function of excitation intensities, using as fitting parameters the time constants and rate coefficients defined in Table II. To describe the buildup and decay kinetics of rare-earth luminescence in a semiconductor host, we assumed only band-band pulse excitation. The above set of ten equations (1)–(10) was reduced to eight dimensionless differential equations which is more convenient for numerical solutions. To solve this system we assumed, for simplicity, that the above band-gap excitations take place at low enough temperatures (in our experiment 8.6 K) so that thermal activation of the trapped carriers is negligible. That is, terms explicitly dependent on temperature were ignored, and only trapping, transferring, and recombination transitions were considered. The radiative recombination of excitons bound to “simple” isoelectronic impurities has a long lifetime ranging from a few hundred to a few thousand nanoseconds.^{24,28–32} That time is much longer than the energy-transfer time τ_{XT} from an exciton bound to a REI trap to core states. The measurements on n -type InP:Yb show that this transfer time is much less than 10 ns.⁷ The above facts explain why we do not observe the luminescence of excitons bound to REI traps. The numerical solution of Eqs. (1)–(10) was obtained using the parameters shown in Table II. Gor-

TABLE II. Parameters describing rise and decay kinetics of InP:Yb.

Symbol	Unit	Parameter value	References
τ_2	s	2×10^{-7}	24,28–32
τ_3	s	11.6×10^{-6}	9,44
τ_{BT}	s	5×10^{-7}	31,32,41–43
τ_{BXT}	s	5×10^{-7}	31,32,41–43
τ_{ns}	s	5×10^{-8}	33(b),33(c)
τ_{ps}	s	3×10^{-8}	33(b),33(c)
τ_{XT}	s	1.25×10^{-9}	7
τ_{et}	s	5×10^{-11}	33(b),33(c)
τ_{px}	s	5×10^{-11}	33(b),33(c)
B_T	cm ³ /s	4×10^{-10}	
B_{FBI}	cm ³ /s	1×10^{-11}	31,32,41–43
B_{BT1}	cm ³ /s	1.2×10^{-13}	31,32,41–43
B_{BT2}	cm ³ /s	1.2×10^{-13}	31,32,41–43
B_{BT3}	cm ³ /s	4×10^{-13}	45–48
B_{BT4}	cm ³ /s	4×10^{-13}	45–48
N_s	cm ⁻³	8×10^{16}	
N	cm ⁻³	5×10^{17}	
G	# photons/(cm ³ s)	$2 \times 10^{20} - 1.5 \times 10^{23}$	

don and Allen^{46(a)} and Ayling and Allen^{46(b)} and Langer, Van Hong^{45,48(a),48(b)} made quantitative measurements of the luminescence efficiency and lifetime in ZnS:Mn, ZnSe:Mn, CdF₂:Mn, and CdF₂:Gd, where they obtained a value for the Auger quenching coefficients by free electrons and an electron bound on shallow donors.⁴⁸ A surprising result is that the value of Auger coefficients for centers in CdF₂ ($\approx 5 \times 10^{-15}$ cm³ s⁻¹) is about four order of magnitude smaller than the value for ZnS and ZnSe (5×10^{-10} cm³ s⁻¹). Klein, Ferneaux, and Henry^{46(c)} estimated the Auger coefficient for the InP:Fe system to be $\approx 6.7 \times 10^{-10}$ cm³ s⁻¹. Excellent reviews of theory and experimental data of Auger processes and values of coefficients are given by Landsberg and Adams.^{42,43} The values of the parameters chosen for the calculations are estimated from experimental data obtained from similar “simple” isoelectronic traps (see references in Table II). We believe that all constants are realistic, and characteristic for InP:Yb. The volume generation range G of e - h pairs was chosen in the same range as in the experiment.⁴⁴ The kinetics of luminescence of InP:Yb as the functions of excitation intensity was simulated by repeating the numerical calculations for several different values of the generation rate. We simulated the kinetics of the photoluminescence measurement by choosing square generating pulses with 60- μ s duration, adequate to establish a quasiequilibrium luminescence intensity during excitation. The luminescence intensities are proportional to N_0^* , N_-^* , and N_X^* . The last two terms can be ignored because they introduce very small contributions to the total luminescence intensity, mainly during the excitation pulse. The numerically simulated luminescence rise and decay are shown in Fig. 6 as a function of generation rates (G), and sets of the parameters from Table II. The profiles shown the buildup of luminescence, allowing the process to reach a steady-state value for a given excitation intensity, and the decay after switching off the exci-

tation pulse. All profiles shown on Fig. 6 are normalized to unity at maximum. The rise times given in the figure decrease with the increasing generation rates. At the low generation rate of 2×10^{20} photon/(cm³s) the buildup curve (which can be well approximated by a single exponential curve) has a rise time of 11.98 μ s, while at the generation rate of 1.5×10^{23} photons/(cm³s) the rise time is 1.7 μ s. The decay profiles for the above two generation rates shown in Fig 6 are 11.7 μ and 6.9 μ s, respectively. The remaining four decay times fall in that window. The rise and decay times for simulated kinetics are well approximated by single exponential processes, while the experimental data are described better by double exponential functions. Figure 7 shows the computed rise and decay times as a function of excitation intensities (generation rate). The experimental data are imposed on the computed curve. The circle shown in Fig. 7 represents experimental rise times obtained from fitting to a single exponential function (with the coefficient of determination $r^2 \approx 0.98$). The squares stand for the rise times of the dominant component of the experimental data fitted to a double exponential function. In Fig. 7 the upper solid line is the computed decay time and the dots represent the experimental decay times of the dominant component of the double exponential fitting. The second small exponential component has the decay times in the range 0.9–1.8 μ s. The double exponential rise and decay times observed in the experiment are probably related to other energy-transfer processes (not incorporated to our model) from Yb to other accidental impurities where the energy is dissipated nonradiatively. Iron is a common contaminant in metal-organic chemical-vapor deposition (MOCVD) grown Yb-doped InP crystals. The energy-transfer process from Yb³⁺ to Fe ions is attributed to thermal quenching of the luminescence intensity and decay time with an increase in temperature.⁴⁴ The detailed analysis of the parameters and their influence on the rise

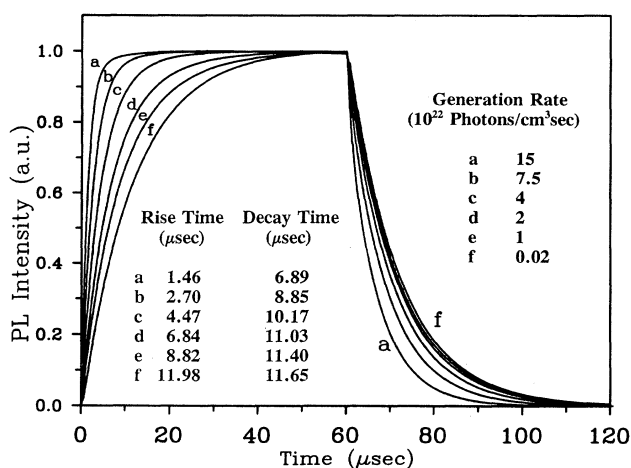


FIG. 6. Numerical solutions of Eqs. (1)–(10). The rare-earth luminescence intensity vs time for different generation rates and the set of parameters shown in Table II. The set of curves a–f represents computed profiles (normalized to unity at maximum), showing the buildup of luminescence, the steady-state value, and the decay after switching off (at 60 μ s) the excitation pulse.

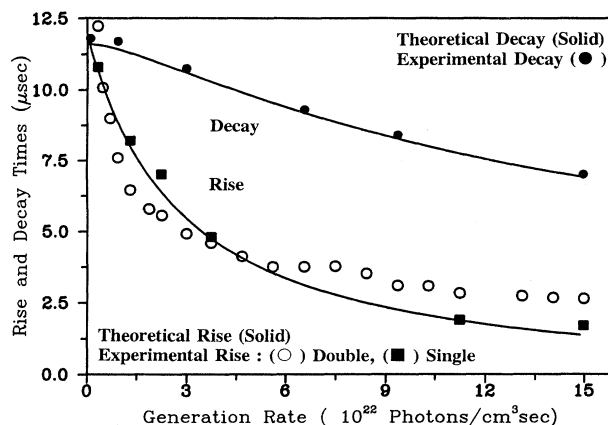


FIG. 7. The numerically computed rise time (solid line) of rare-earth luminescence (InP:Yb) as a function of generation rates. The circles represent the experimental values of the rise-time constants of ytterbium luminescence in InP at 8.4 K (fitted to single exponential function, with the coefficient of determination $r^2 \approx 0.98$). The squares stand for the rise-time constants of the dominant component of the experimental data fitted to the double exponential function. The dots stand for the decay-time constants of the dominant component of the experimental data fitted to double exponential function.

time, and the efficiency of the steady-state luminescence and decay time will be published elsewhere. The numerically simulated luminescence rise and decay measurements show a good overall quantitative agreement with the experiment over a wide range of generation rates (Figs. 6 and 7). Finally, the proposed model can be refined by taking into account the surface recombination and carrier diffusion processes, which may play important roles in the reduction of the overall photoluminescence emission.⁵³

IV. POSSIBLE QUENCHING MECHANISMS AND TEMPERATURE DEPENDENCE

Discussed below are several possible nonradiative processes that quantitatively explain the kinetics (rise and decay of luminescence of the REI trap) and temperature dependence of the observed quenching. The Auger quenching processes defined in Sec. III are shown in Figs. 3–5. Processes [Figs. 4(a) and 4(b) and 5(a) and 5(b)] nonradiative recombination involving the interaction of a core excited REI trap, with an electron trapped on a separate REI trap. The next two-center recombination involves the interaction of the excited REI trap with an electron (hole) on a separate neutral donor (acceptor), respectively. The rate equations describe the nonradiative recombination involving the interaction of a core excited REI trap, with a free electron or hole, respectively. The last process is a very efficient nonradiative deexcitation mechanism of localized centers (Mn²⁺) in ZnS, ZnSe, and CdF₂^{45,47} and Gd³⁺ and Tb³⁺ in CdF₂.⁴⁸ The free-carrier Auger quenching processes are important at higher temperatures, and were shown to be much more efficient than the Auger process due to the shallow

donors. The last one is important only at low temperatures.⁴⁷ The most probable nonradiative mechanism quenching the rare-earth luminescence in III-V semiconductors is the Auger energy back transfer mechanism shown schematically in Figs. 3(a) and 3(b). The rare-earth-excited isoelectronic trap occupied by electron N_X^* or exciton N_X^* can transfer energy to the trapped electron or exciton rather than to the radiative field; the electron is consequently ejected deep into the conduction band. It is emphasized that at low temperatures the only electrons in the conduction band come from either the exciting source or from Auger ionization of the REI traps or neutral donors (in the case of n -type samples). The nonradiative recombination involving the interaction of the corexited REI trap with a free electron (or hole) is important in seminsulating InP crystals only during the excitation pulse. In the dark the electron concentration at a temperature of 300 K is in the range $1 \times 10^8 \text{ cm}^{-3}$. However, the experimental decay time of Yb luminescence is $\sim 12 \mu\text{s}$ in SI-, n -, and p -type InP:Yb.^{3,4,6}

The other mechanisms of the nonradiative recombination of the excited states of localized centers in semiconductors are first, the multiphonon relaxation processes,⁵⁵ and second, a migration of energy and cross relaxation processes.^{56,57} The probability of the multiphonon relaxation processes is dependent upon the type of coupling with the lattice vibrations and the phonon frequency distribution. The ion-host lattice interaction for $\text{RE}^{3+} 4f^n$ electrons is characteristic of weak coupling, and the multiphonon emission rates exhibit an approximately exponential dependence on the energy gap to the next lowest level. For a single frequency p phonon process the nonradiative rate for narrow-line emission is described by Kiel's formula⁵⁸

$$W_{nr}^p(T) = W_{nf}^p(0)[1+n]^p,$$

where $W_{nf}^p(0)$ is the rate at low temperature, p is the number of phonons involved, n is the occupancy of the phonon modes:

$$n = [\exp(\hbar\omega/kT) - 1]^{-1},$$

and the average phonon energy $\hbar\omega = \Delta E/p$. The single frequency model seems to be an oversimplification, and taking a weighted average over the phonon's spectrum, or consideration of the continuous nature of the phonon spectrum would be more appropriate.⁵⁹

The results of many studies demonstrate that for given host crystals, the most critical parameter affecting the rate of multiphonon emission is the energy gap to the nearest-lower level. If the energy gap to the next lower state is sufficiently large the nonradiative multiphonon rate is negligible compared to the radiative rate, and this is the situation for most rare-earth ions in III-V semiconductors. For example, in InP: Yb³⁺ the ${}^2F_{3/2} - {}^2F_{7/2}$ energy gap is 9895 cm^{-1} , in GaAs: Er³⁺ the ${}^4I_{13/2} - {}^4I_{15/2}$ energy gap is 6051 cm^{-1} , and in GaAs:Nd³⁺ the ${}^4F_{3/2} - {}^4I_{11/2}$ energy gap is $10\,636 \text{ cm}^{-1}$. The highest energy phonons in InP and GaAs are 345.2 and 292.7 cm^{-1} LO phonons, respectively. Nonradiative decay for the three cases above would require the generation of 27, 21,

and 36 LO phonons, respectively. Studies in different host materials,^{55(a),55(b)} show that nonradiative decay involving the generation of more than five phonons is weaker than the radiative process.

When the concentrations of the rare-earth luminescent ions are higher, or centers create pairs, allowance must be made of the possibility of interaction between centers. This interaction may be too weak to modify the energy levels, but yet be adequately strong to enable transfer of energy from one to another.^{38(b),57}

The migration of energy in InP doped with Yb³⁺ occurs through resonant interaction. The energy level diagram of Yb³⁺ in a crystal field of the tetrahedral symmetry (T_d) in InP indicates that the only possible interaction between the Yb³⁺ ions at low temperature is resonant interaction between the lower Stark sublevel of the ground state ${}^2F_{7/2}$ and the lower Stark to the accidental impurity with an absorption spectrum overlapping with that of the Yb³⁺ ion, emission is the most probable quenching mechanism. In Nd³⁺-doped GaAs the energy of a single excited ion may be transferred to the same level of an identical ion (resonant energy migration), and finally to the quenching center.^{52,54,60,61,44} The second possible degradation of excitation energy is the cross relaxation process. The presence of appropriate intermediate levels in the Nd³⁺ ion (${}^4I_{11/2}$ and ${}^4I_{13/2}$) between the ground ${}^4I_{9/2}$ and excited ${}^4I_{3/2}$ states makes effective the cross relaxation process and increases the probability of nonradiative quenching processes.^{38,62,63} All the above-discussed transfer processes are temperature dependent and can be useful in explaining the quenching of luminescence of rare earths in semiconductors. A full account of our results on the temperature dependence of rise, decay, and quenching mechanisms will be published at a latter date.

V. SUMMARY

In this work we have developed a kinetics model of energy transfer from the host lattice to the localized core excited states of rare-earth isoelectronic structured traps. According to Robbins and Dean¹⁷ the formation of bound states at the structured cationic isoelectronic impurities is fairly common, which is in contrast to the situation normally found for anionic substituents in semiconductors. The outer electron configurations of RE^{3+} ions are the same ($5s^25p^6$). Among rare-earth ions are those that, upon replacing the element from column III in III-V compounds that are isovalent concerning outer electrons of RE^{3+} ions, create isoelectronic traps in III-V semiconductors. We have evidence that the other RE ions in III-V semiconductors can occupy different sites (not only substitutional). The rare-earth isoelectronic trap must not necessarily be the "pure" substitutional center; if the rare-earth ions are very active chemically, they can create a more complex center involving other impurity or native defects. This conclusion is supported by the fact that the atomic covalent radii (ionic RE^{3+}) for all rare earths are bigger than atomic radii of Ga in In that they replace. Pauling's electronegativity of rare-earth elements are in the range of 1.1–1.25, and are

smaller than Ga (1.81) and In (1.78) for which they substitute. The rare-earth isovalent traps that we can call isoelectronic "structured" impurities¹⁷ possess the unfilled $4f^n$ core shell. The structured luminescence arises from intraconfiguration f - f transitions in the core of the isoelectronic "structured" impurities.

The presence of low-lying empty core orbitals in rare-earth impurities introduces new excitation and recombination phenomena. To adequately describe the energy transfer to the REI trap, and the buildup and decay kinetics of rare-earth luminescence, we have considered six separate states of the REI impurity (unoccupied, electron occupied, electron occupied excited, neutral exciton occupied, excited electron occupied, and excited exciton occupied). The energy-transfer processes occur through an Auger mechanism, where the recombination energy of the bound electron with the free hole is transferred non-radiatively to the core states. The second energy-transfer process is the transfer of energy from the bound exciton on the REI trap to the core states. If the initial and final states are not resonant (in both mechanisms), the energy mismatch must be accommodated by emission or absorption of phonons.^{17,38(b),56} Furthermore, we discussed the details of several quenching processes which are incorporated into the kinetics equations. We derive two sets of differential equations for SI-, and n - (p -) type semiconductors governing the kinetics of rare-earth luminescence. The nonradiative pathways present alternative recombination possibilities for the electrons and holes and are incorporated in both models. Equations governing the transfer of energy processes and recombination kinetics have been determined and solved by a numerical method

to derive the time dependence of the rise and decay kinetics as a function of excitation intensity. The parameters used are realistic, but only approximately known (see Table II). The numerically simulated luminescence rise and decay times show a good overall quantitative agreement with experiment over a wide range of generation rate values (see Figs. 6 and 7). Finally, the proposed model can be refined by taking into account the quenching processes discussed above, and the surface recombination and carrier diffusion processes, which plays an important role in reduction of the overall photoluminescence emission.⁵³

ACKNOWLEDGMENTS

The author would like to thank D. C. Reynolds and D. C. Look from Wright Laboratory Wright-Patterson AFB Dayton, OH, and K. Takahei, M. Taniguchi, and A. Taguchi from NTT for several helpful discussions during his sabbatical leave at Wright Laboratory, and at NTT Basic Research Laboratories, Tokyo. The author thanks G. S. Pomrenke, S. Ulloa, and R. L. Cappelletti for critical reading of this manuscript. This research is funded by AFOSR (Grant No. 90-0322).

APPENDIX

Consulting Figs. 1-5, the equations describing the transfer and recombination kinetics in n -type semiconductor may be written as follows:

$$\begin{aligned} \frac{dN_-}{dt} = & \frac{n}{\tau_{et}} \left[\frac{N_0}{N} \right] + \frac{N^*}{\tau_3} + \frac{1}{\tau_{xp}} \left[\frac{N_X}{N} \right] \frac{N_v}{\beta_h} \exp \left[-\frac{E_h}{kT} \right] - \frac{1}{\tau_{te}} \left[\frac{N_-}{N} \right] \beta_t N_c \exp \left[-\frac{E_t}{kT} \right] \\ & - \frac{p}{\tau_{px}} \left[\frac{N_-}{N} \right] - B_{FBI}(N_-)p - B_{BT1}N_0^*(N_-) - B_T(N_-)p, \end{aligned} \quad (A1)$$

$$\frac{dN_X}{dt} = \frac{N_X^*}{\tau_3} + \frac{p}{\tau_{px}} \left[\frac{N_-}{N} \right] - N_X \left[\frac{1}{\tau_2} + \frac{1}{\tau_{XT}} + \frac{1}{\tau_{xd}} \right] - \frac{1}{\tau_{xp}} \left[\frac{N_X}{N} \right] \frac{N_v}{\beta_h} \exp \left[-\frac{E_h}{kT} \right], \quad (A2)$$

$$\begin{aligned} \frac{dN_0^*}{dt} = & \frac{N_X}{\tau_{XT}} + B_T(N_-)p + \frac{1}{\tau_{te}} \left[\frac{N_-}{N} \right] \beta_t N_c \exp \left[-\frac{E_t}{kT} \right] - \frac{n}{\tau_{et}} \left[\frac{N_0^*}{N} \right] - \frac{N_0^*}{\tau_3} \\ & - B_{BT5}(N_D^0)(N_0^*) - B_{BT1}(N_-)(N_0^*) - B_{BT3}(n)(N_0^*) - B_{BT4}(p)(N_0^*) \end{aligned} \quad (A3)$$

$$\begin{aligned} \frac{dN_-^*}{dt} = & \frac{n}{\tau_{et}} \left[\frac{N_0^*}{N} \right] + \frac{1}{\tau_{xp}} \left[\frac{N_X^*}{N} \right] \frac{N_v}{\beta_h} \exp \left[-\frac{E_h}{kT} \right] - N_-^* \left[\frac{1}{\tau_3} + \frac{1}{\tau_{BT}} \right] - B_{FBI}(N_-^*)p \\ & - \frac{p}{\tau_{px}} \left[\frac{N_-^*}{N} \right] - \frac{1}{\tau_{te}} \left[\frac{N_-^*}{N} \right] \beta_t N_c \exp \left[-\frac{E_t}{kT} \right] - B_{BT2}(N_0^*)(N_-^*), \end{aligned} \quad (A4)$$

$$\frac{dN_X^*}{dt} = \frac{p}{\tau_{px}} \left[\frac{N_-^*}{N} \right] - N_X^* \left[\frac{1}{\tau_2} + \frac{1}{\tau_3} + \frac{1}{\tau_{BXT}} + \frac{1}{\tau_{xd}} \right] - \frac{1}{\tau_{xp}} \left[\frac{N_X^*}{N} \right] \frac{N_v}{\beta_h} \exp \left[-\frac{E_h}{kT} \right], \quad (A5)$$

$$\begin{aligned} \frac{dn}{dt} = & G + N_X^* \left[\frac{1}{\tau_{xd}} + \frac{1}{\tau_{BXT}} \right] + \left[\frac{N_- + N_-^*}{N} \right] \frac{1}{\tau_{te}} \beta_t N_c \exp \left[-\frac{E_t}{kT} \right] + \frac{N_X}{\tau_{xd}} + \frac{N_-^*}{\tau_{BT}} - \frac{n}{\tau_{et}} \left[\frac{N_0 + N_0^*}{N} \right] - \frac{n}{\tau_{ns}} \left[\frac{N_s^0}{N_s} \right] \\ & + B_{BT1}(N_-)(N_0^*) + B_{BT5}(N_0^*)N_D^0 + \left[\frac{N_D^0}{N_D} \right] \frac{N_c}{\tau_{nD}} \beta_D \exp \left[-\frac{E_D}{kT} \right] - \left[1 - \frac{N_D^0}{N_D} \right] \frac{n}{\tau_{nD}} + B_{BT2}(N_0^*)N_-^* , \end{aligned} \quad (A6)$$

$$\frac{dp}{dt} = G + \frac{p_h}{\tau_{xp}} \left[\frac{N_X}{N} \right] + \frac{p_h}{\tau_{xp}} \left[\frac{N_X^*}{N} \right] - \frac{p}{\tau_{px}} \left[\frac{N_-}{N} \right] - \frac{p}{\tau_{px}} \left[\frac{N_-^*}{N} \right] - B_{FBI}(N_- + N_-^*)p - \frac{p}{\tau_{ps}} \left[\frac{N_s - N_s^0}{N_s} \right] - B_{FBD}(N_D^0)p , \quad (A7)$$

$$\frac{dN_s^0}{dt} = \frac{p}{\tau_{ps}} \left[1 - \frac{N_s^0}{N_s} \right] - \frac{n}{\tau_{ns}} \left[\frac{N_s^0}{N_s} \right] , \quad (A8)$$

$$\frac{dN_D^0}{dt} = \left[1 - \frac{N_D^0}{N_D} \right] \frac{n}{\tau_{nD}} - \left[\frac{N_D^0}{N_D} \right] \frac{\beta_D N_c}{\tau_{nD}} \exp \left[-\frac{E_D}{kT} \right] - B_{BT5}(N_D^0)N_0^* - B_{FBD}(N_D^0)p , \quad (A9)$$

$$N_0 = N - N_- - N_X - N_0^* - N_-^* - N_X^* ,$$

$$N_s = N_s^0 + N_s^- ,$$

$$N_D = N_D^0 + N_D^+ ,$$

$$p + N_D^+ = n + N_- + N_-^* + \left[1 - \frac{N_s^0}{N_s} \right] N_s .$$

Finally, the equation indicating the neutrality condition is

$$p = n + N_- + N_-^* + \left[1 - \frac{N_s^0}{N_s} \right] N_s - \left[1 - \frac{N_D^0}{N_D} \right] N_D \quad (A11)$$

Equations (A1)–(A5) govern the negatively charged REI-trap population (A1), the neutral exciton occupied REI-trap population (A2), the neutral core excited REI-trap population (A3), the negatively charged core excited REI-trap population (A4), and the exciton occupied core excited (A5) rare-earth isoelectronic trap populations, respectively. Equations (A6) and (A7) represent the changes in the total free-electron and hole populations, respectively. Equation (A8), governs the density of neutral shunt path traps. Equation (A9) governs the density of neutral donors. Equations (A10) state the constancy of the total concentrations of REI traps, shunt paths, and donors, respectively, and Eq. (A11) is the neutrality condition equation. The symbols used in this set of equations are the same as for SI semiconductors.

¹H. Ennen, G. Pomrenke, and A. Axmann, *J. Appl. Phys.* **57**, 2182 (1985).

²G. Aszodi, J. Weber, Ch. Uihlein, L. Pu-lin, H. Ennen, U. Kaufmann, J. Schneider, and J. Windschweif, *Phys. Rev.* **31**, 7767 (1985).

³P. B. Klein, *Solid State Commun.* **65**, 1097 (1988).

⁴V. I. Masterov and L. F. Zakharenkov, *Fiz. Tekh. Polopruvudu*, **24**, 610 (1990), and references cited therein.

⁵(a) P. S. Whitney, K. Uwai, H. Nakagome, and K. Takahei, *Appl. Phys. Lett.* **53**, 2074 (1988); (b) K. Takahei and A. Taguchi, in *Materials Science Forum*, edited by G. Davies, G. DeLeo, and M. Stavola (Trans Tech, Zürich, Switzerland, 1992), Vols. 83–87, p. 641, and references therein; (c) M. Godlewski, K. Swiatek, A. Suchocki, and J. M. Langer, *J. Lumin.* **48&49**, 23 (1991).

⁶K. Thonke, K. Pressel, G. Bohnert, A. Stapor, J. Weber, M. Moser, A. Malassioti, A. Hangleiter, and F. Scholz, *Semicond. Sci. Technol.* **5**, 1124 (1990).

⁷C. Lhomer, B. Lambert, Y. Toudic, A. Le Corre, M. Gauneau, F. Clerot, and B. Sermage, *Semicond. Sci. Technol.* **6**, 916 (1991).

⁸A. Taguchi, H. Nakagome, and K. Takahei, *J. Appl. Phys.* **70**, 5604 (1991).

⁹H. J. Lozykowski, A. K. Alshawa, G. Pomrenke, and I. Brown, *Bull. Am. Phys. Soc.* **36**, 2167 (1991).

¹⁰J. Wagner, J. Windschweif, and H. Ennen, *Phys. Rev. B* **30**, 6230 (1984).

¹¹A. Stapor, J. Raczyńska, H. Przybylinska, K. Fronc, and J. M. Langer, in *Material Science Forum*, edited by H. J. von Bardeleben (Trans Tech, Zürich, Switzerland, 1986), Vols. 10–12, p. 633.

¹²(a) D. Seghier, T. Benyattou, G. Bremond, F. Ducroquet, J. Gregoire, G. Guillot, C. Lhomer, B. Lambert, Y. Toudic, and A. Le Corre, *Appl. Phys. Lett.* **60**, 983 (1992); (b) B. Lambert, A. Le Corre, Y. Toudic, C. Lhomer, G. Grandpierre, and M. Gauneau, *J. Phys. Condens. Matter.* **2**, 479 (1990); (c) S. N. Mustafaeva and M. M. Asadov, *Inorg. Matter.* **25**, 180 (1989); (d) A. Taguchi, H. Nakagome, and K. Takahei, *J. Appl. Phys.* **68**, 330 (1990); (e) J. E. Colon, D. W. Elsaesser, Y. K. Yeo, R. L. Hengehold, and G. S. Pomrenke, in *Material Science Forum* [Ref. 5(b)], Vols. 83–87, p. 671.

¹³(a) T. Benyattou, D. Seghier, G. Guillot, R. Moncorge, P. Gal-

- tier, and M. N. Charasse, in *Impurities, Defects and Diffusion in Semiconductors: Bulk and Layered Structures*, edited by D. J. Wolford, J. Bernholc, and E. E. Maller, MRS Symposia Proceedings No. 163 (Materials Research Society, Pittsburgh, 1990); p. 69; (b) T. Benyattou, D. Seghier, G. Guillot, R. Moncorge, P. Galtier, and M. N. Charasse, *Appl. Phys. Lett.* **58**, 2132 (1991).
- ¹⁴A. C. Aten, J. H. Haanstra, and H. de Vries, *Philips Res. Rep.* **20**, 395 (1965).
- ¹⁵D. G. Thomas, *J. Phys. Soc. Jpn.* **21**, 265 (1966).
- ¹⁶D. G. Thomas, J. J. Hopfield, and C. J. Frosch, *Phys. Rev. Lett.* **15**, 857 (1965).
- ¹⁷D. J. Robbins and P. J. Dean, *Adv. Phys.* **27**, 499 (1978), and references therein.
- ¹⁸H. C. Casey, Jr. and G. L. Pearson, *J. Appl. Phys.* **35**, 3401 (1964).
- ¹⁹J. W. Allen, *J. Phys. C* **4**, 1936 (1971).
- ²⁰A. Baldereschi and J. J. Hopfield, *Phys. Rev. Lett.* **28**, 171 (1972).
- ²¹A. Baldereschi, *J. Lumin.* **7**, 79 (1973).
- ²²P. J. Dean, *J. Lumin.* **7**, 51 (1973).
- ²³W. Czaja, in *Advances in Solid State Physics XI*, edited by O. Madelung (Pergamon, New York, 1971) p. 65, and references therein.
- ²⁴P. J. Dean, A. M. White, E. W. Williams, and M. G. Astles, *Solid State Commun.* **9**, 1555 (1971).
- ²⁵W. Ruhle, W. Schmid, R. Meck, N. Stath, J. U. Fischbach, I. Strottner, K. W. Benz, and M. Pilkuhn, *Phys. Rev. B* **18**, 7022 (1978).
- ²⁶J. L. Merz and R. T. Lynch, in *II-VI Semiconducting Compounds*, edited by D. G. Thomas (Benjamin, New York, 1967), p. 730.
- ²⁷(a) H. J. Lozykowski, P. O. Holtz, and B. Monemar, *J. Electron. Mater.* **12**, 653 (1983); (b) H. J. Lozykowski and J. L. Merz, in *Properties of II-VI Semiconductors: Bulk Crystals, Epitaxial Films, Quantum Well Structures, and Dilute Magnetic Systems*, edited by F. J. Bartoli, Jr., H. F. Schaalier, and J. F. Schetzina, MRS Symposia Proceedings No. 161 (Materials Research Society, Pittsburgh, 1990), p. 171.
- ²⁸T. R. N. Kutty and R. Revathi, *Solid State Commun.* **55**, 197 (1985).
- ²⁹J. D. Cuthbert and D. G. Thomas, *Phys. Rev.* **154**, 763 (1967).
- ³⁰J. D. Cuthbert, C. H. Henry, and P. J. Dean, *Phys. Rev.* **170**, 739 (1968).
- ³¹J. S. Jayson, R. N. Bhargava, and R. W. Dixon, *J. Appl. Phys.* **41**, 4972 (1970).
- ³²J. M. Dishman and M. DiDomenico, Jr., *Phys. Rev. B* **1**, 3381 (1970); J. M. Dishman, M. DiDomenico, Jr., and R. Caruso, *ibid.* **2**, 1988 (1970); R. H. Bube, *J. Phys. Chem. Solids*, **1**, 234 (1957).
- ³³(a) J. S. Jayson and R. Z. Bachrach, *Phys. Rev. B* **4**, 477 (1971); (b) M. Sternheim and E. Cohen, *Solid-State Electron.* **21**, 1343 (1978); (c) *Phys. Rev. B* **22**, 1875 (1980).
- ³⁴(a) U. Heim, *Phys. Status Solidi B* **48**, 629 (1971), (b) C. J. Hwang and L. R. Dawson, *Solid State Commun.* **10**, 443 (1972).
- ³⁵*Table of Periodic Properties of the Elements* (Sargent-Welch, Skokie, IL, 1980).
- ³⁶J. C. Phillips, *Bonds and Bands in Semiconductors* (Academic, New York, 1973), p. 54.
- ³⁷J. Shaffer and F. Williams, *Phys. Status Solidi* **38**, 657 (1970).
- ³⁸For a review, see (a) D. L. Huber, in *Laser Spectroscopy of Solids*, edited by W. M. Yen and P. M. Selzer (Springer-Verlag, Berlin, 1981), p. 83; (b) T. Holstein, S. K. Lyo, and R. Orbach, *ibid.*; p. 39.
- ³⁹P. D. Dapkus, W. H. Hackett, Jr., O. G. Lorimor, and R. Z. Bachrach, *J. Appl. Phys.* **45**, 4920 (1974).
- ⁴⁰R. Z. Bachrach and O. G. Lorimor, *J. Appl. Phys.* **43**, 500 (1972).
- ⁴¹J. M. Dishman, *Phys. Rev.* **3**, 2588 (1971); K. P. Sinha and M. DiDomenico, Jr., *Phys. Rev. B* **1**, 2623 (1970).
- ⁴²P. T. Landsberg and M. J. Adams, *J. Lumin.* **7**, 3 (1973).
- ⁴³P. T. Landsberg, *Recombination in Semiconductors* (Cambridge University Press, Cambridge, 1991), and references cited therein.
- ⁴⁴H. J. Lozykowski, A. K. Alshawa, G. S. Pomrenke, and I. Brown, in *Rare Earth Doped Semiconductors*, edited by G. S. Pomrenke, P. B. Klein, and D. W. Langer, MRS Symposia Proceedings Vol. 301 (Materials Research Society, Pittsburgh, 1993), p. 263.
- ⁴⁵J. M. Langer, in *Electroluminescence*, edited by S. Shinoya and H. Kobayashi, Springer Proceedings in Physics Vol. 38 (Springer-Verlag, Berlin, 1989), and references cited therein.
- ⁴⁶(a) N. T. Gordon and J. W. Allen, *Solid State Commun.* **37**, 441 (1981); (b) S. G. Ayling and J. W. Allen, *J. Phys. C* **20**, 4251 (1987); (c) P. B. Klein, J. E. Furneaux, and R. L. Henry, *Phys. Rev. B* **29**, 1947 (1984).
- ⁴⁷A. Suchocki and J. M. Langer, *Phys. Rev. B* **39**, 7905 (1989).
- ⁴⁸(a) J. M. Langer, *J. Lumin.* **23**, 141 (1981). (b) J. M. Langer and Le Van Hong, *J. Phys. C* **17**, L923 (1984).
- ⁴⁹E. W. Williams and H. B. Bebb, in *Semiconductors and Semimetals*, edited by R. K. Willardson and A. C. Beer (Academic, New York, 1972), Vol. 8, Chap. 5, p. 321, and references cited therein.
- ⁵⁰E. I. Tolpygo, K. B. Tolpygo, and M. K. Sheinkman, *Fiz. Tverd. Tela (Leningrad)* **7**, 1790 (1965) [*Sov. Phys. Solid State* **7**, 1442 (1965)].
- ⁵¹G. F. Neumark, D. J. DeBitetto, R. N. Bhargava, and P. M. Harnack, *Phys. Rev. B* **15**, 3147 (1977); **1**, 3156 (1977).
- ⁵²M. J. Weber, *Phys. Rev. B* **4**, 2932 (1971).
- ⁵³M. Boulou and D. Bois, *J. Appl. Phys.* **48**, 4713 (1977).
- ⁵⁴J. P. van der Ziel, L. Kopf, and L. G. Van Uitert, *Phys. Rev. B* **6**, 615 (1972).
- ⁵⁵(a) H. W. Moss, *J. Lumin.* **1-2**, 106 (1970); (b) L. A. Riseberg and M. J. Weber, in *Progress in Optics*, edited by E. Wolf (North-Holland, Amsterdam, 1975), Vol. 14.
- ⁵⁶For a review, see (a) R. K. Watts, in *Optical Properties of Ionic Solids*, edited by B. DiBartolo (Plenum, New York, 1975), pp. 307-336; (b) B. Henderson and G. F. Imbusch, *Optical Spectroscopy of Inorganic Solids* (Oxford University Press, New York, 1989).
- ⁵⁷G. P. Morgan and W. M. Yen, in *Laser Spectroscopy of Solids II*, edited by W. M. Yen (Springer-Verlag, Berlin, 1989), p. 77.
- ⁵⁸A. Kiel, in *Proceedings of the Third International Conference on Quantum Electronics, Paris, 1963*, edited by P. Grivet and N. Bloembergen (Columbia University Press, New York, 1964).
- ⁵⁹M. D. Sturge, *Phys. Rev. B* **8**, 6 (1973).
- ⁶⁰B. A. Wilson, W. M. Yen, J. Hagarty, and G. F. Imbusch, *Phys. Rev. B* **19**, 4238 (1979).
- ⁶¹F. Kellendonk, and G. Blasse, *J. Chem. Phys.* **75**, 561 (1981).
- ⁶²Yu. K. Voron'ko, V. V. Osiko, N. V. Savost'yanova, V. S. Fedorov, and I. A. Shcherbakov, *Fiz. Tverd. Tela (Leningrad)* **14**, 2656 (1973) [*Sov. Phys. Solid State* **14**, 2294 (1973)].
- ⁶³H. J. Lozykowski and K. Takahei (unpublished).